ACS OMEGA

Article

Cite This: ACS Omega 2019, 4, 4348−4359

http://pubs.acs.org/journal/acsodf

A FRET-Based Fluorogenic Trehalose Dimycolate Analogue for Probing Mycomembrane-Remodeling Enzymes of Mycobacteria

Nathan J. Holmes,[†,⊥] Herbert W. Kavunja,[†,⊥] Yong Yang,[‡] B. Dillon Vannest,[†] Claudia N. Ramsey,[†] Dana M. Gepford,[†] Nicholas Banahene,[†] Anne W. Poston,[†] Brent F. Piligian,[†] Donald R. Ronning,[§] Anil K. Ojha,[‡,∥] and Benjamin M. Swarts*[,†]

[†]Department of Chemistry and Biochemistry, Central Michigan University, Mount Pleasant, Michigan 48859, United States

[‡]Division of Genetics, Wadsworth Center, New York State Department of Health, Albany, New York 12208, United States

[§]Department of Chemistry and Biochemistry, University of Toledo, Toledo, Ohio 43606-3390, United States

[∥]Department of Biomedical Sciences, University at Albany, New York 12208, United States

Supporting Information

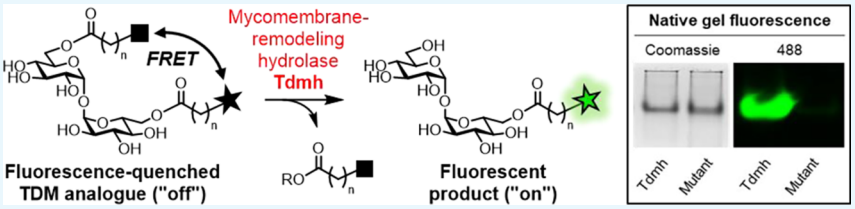

ABSTRACT: The mycobacterial outer membrane, or mycomembrane, is essential for the viability and virulence of *Mycobacterium tuberculosis* and related pathogens. The mycomembrane is a dynamic structure, whose chemical composition and biophysical properties can change during stress to give an advantage to the bacterium. However, the mechanisms that govern mycomembrane remodeling and their significance to mycobacterial pathogenesis are still not well characterized. Recent studies have shown that trehalose dimycolate (TDM), a major glycolipid of the mycomembrane, is broken down by the mycobacteria-specific enzyme TDM hydrolase (Tdmh) in response to nutrient deprivation, a process which appears to modulate the mycomembrane to increase nutrient acquisition, but at the expense of stress tolerance. Tdmh activity thus balances the growth of *M. tuberculosis* during infection in a manner that is contingent upon host immunity. Current methods to probe Tdmh activity are limited, impeding the development of inhibitors and the investigation of the role of Tdmh in bacterial growth and persistence. Here, we describe the synthesis and evaluation of FRET-TDM, which is a fluorescence-quenched analogue of TDM that is designed to fluoresce upon hydrolysis by Tdmh and potentially other trehalose ester-degrading hydrolases involved in mycomembrane remodeling. We found that FRET-TDM was efficiently activated in vitro by recombinant Tdmh, generating a 100-fold increase in fluorescence. FRET-TDM was also efficiently activated in the presence of whole cells of *Mycobacterium smegmatis* and *M. tuberculosis*, but the observed signal was predominantly Tdmh-independent, suggesting that physiological levels of Tdmh are low and that other mycobacterial enzymes also hydrolyze the probe. The latter notion was confirmed by employing a native protein gel-based fluorescence assay to profile FRET-TDM-activating enzymes from *M. smegmatis* lysates. On the other hand, FRET-TDM was capable of detecting the activity of Tdmh in cells when it was overexpressed. Together, our data demonstrate that FRET-TDM is a convenient and sensitive in vitro probe of Tdmh activity, which will be beneficial for Tdmh enzymatic characterization and inhibitor screening. In more complex samples, for example, live cells or cell lysates, FRET-TDM can serve as a tool to probe Tdmh activity at elevated enzyme levels, and it may facilitate the identification and characterization of related hydrolases that are involved in mycomembrane remodeling. Our study also provides insights as to how the structure of FRET-TDM or related fluorogenic probes can be optimized to achieve improved specificity and sensitivity for detecting mycobacteria.

INTRODUCTION

The mycomembrane is a glycolipid-rich outer membrane that is recognized as the defining ultrastructural feature of mycobacteria and related species in the Corynebacterineae suborder.[1,2] These bacteria, which include the devastating intracellular pathogen *Mycobacterium tuberculosis* (*Mtb*),[3] rely on the mycomembrane to permit entry of nutrients into the cell while also providing defense from environmental assaults, such as the host immune response and antibiotic treatment.[4−8] Understanding how mycobacteria modulate their mycomembrane to balance nutrient acquisition, stress tolerance, and immunoactivity will provide insight into how these pathogens thrive in the host at

Received: January 14, 2019
Accepted: February 12, 2019
Published: February 27, 2019

DOI: 10.1021/acsomega.9b00130
ACS Omega 2019, 4, 4348−4359

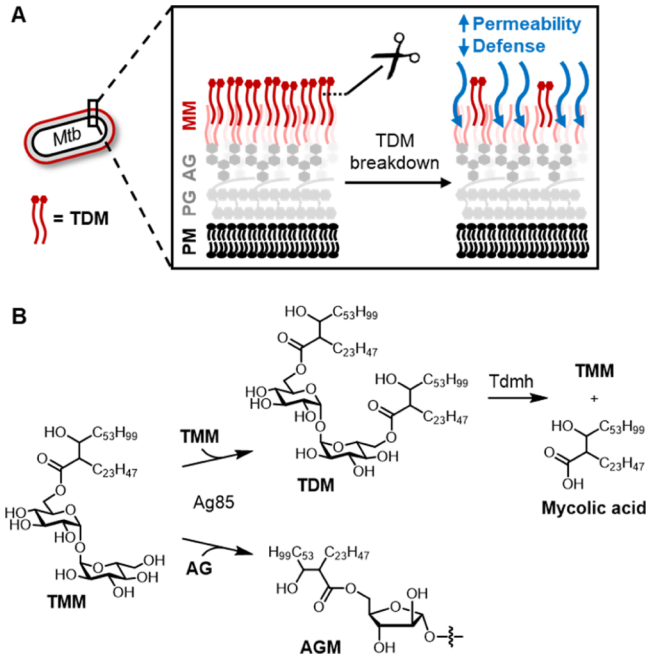

Figure 1. (A) Simplified model for mycomembrane remodeling in *Mtb*. TDM breakdown may modulate mycomembrane permeability, stress tolerance, and immunogenicity. AG, arabinogalactan; MM, mycomembrane; PG, peptidoglycan; PM, plasma membrane. (B) Biosynthesis and breakdown of TDM. TDM is synthesized by Ag85-mediated transfer of a mycoloyl group from one molecule of trehalose monomycolate (TMM) to another. Ag85 also synthesizes AGM using TMM as a mycoloyl donor and AG as an acceptor. TDM is degraded by Tdmh-catalyzed hydrolysis to produce free mycolic acid and TMM (shown) and/or trehalose.

different stages of infection, potentially informing the development of new strategies for tuberculosis diagnosis and treatment.

The mycomembrane is composed of structurally heterogeneous lipid entities including glycolipids, among which sugar esters of branched mycolic acids (C_{30}–C_{100}, depending on the species) are predominant (schematic shown in Figure 1A).[9] The inner leaflet of the mycomembrane is composed of mycolic acids that are ester-linked to arabinofuranosyl units of the underlying arabinogalactan (AG) layer, which in turn is covalently linked to the peptidoglycan layer.[10] The outer leaflet of the mycomembrane is thought to be composed of noncovalently associated lipids and glycolipids, including trehalose dimycolate (TDM), which has mycolic acids esterified to both 6-positions of the disaccharide trehalose (Figure 1B).[10] TDM is an abundant mycobacterial glycolipid, and it has an intriguing dual biological role: it is a major component of the cell envelope that confers structural integrity and stress tolerance to the bacterium, while also serving as a potent immunostimulant that drives key aspects of the host immune response to *Mtb* infection, including granuloma formation.[11−16]

Mounting evidence suggests that, to provide an advantage in certain environments, mycobacteria remodel their mycomembrane by adjusting TDM levels. Known TDM biosynthesis and degradation pathways are depicted in Figure 1B. TDM is biosynthesized by the antigen 85 (Ag85) complex, which consists of several mycoloyltransferase isoforms that catalyze the transfer of mycoloyl groups from TMM to acceptor molecules, including a reaction in which two TMM molecules combine to generate one molecule each of TDM and trehalose.[17−19] While the only established role of Ag85 mycoloyltransferases in vivo is in the synthesis of TDM and AG-linked mycolate (AGM), Ag85-catalyzed breakdown of TDM, via both acyltransferase and acylhydrolase activity, has been observed in assays utilizing purified Ag85 enzyme.[20] Ojha and co-workers recently discovered a dedicated TDM-specific hydrolase (Tdmh), which degrades TDM to release free mycolic acid.[21−23] Studies using *Mycobacterium smegmatis* (*Msmeg*) and *Mtb* mutants lacking Tdmh have provided insights into how TDM levels are regulated to alter mycobacterial physiology and pathogenesis. In nonpathogenic *Msmeg*, Tdmh releases free mycolic acid from TDM during the formation of drug-tolerant biofilms, and the genetic removal of Tdmh retards *Msmeg* biofilm formation.[21] In pathogenic *Mtb*, Tdmh is induced during nutrient deprivation and degrades TDM to increase permeability of the cell envelope toward nutrients, while concomitantly lowering the bacterium's defenses and sensitizing it to stress (Figure 1A).[23] It is proposed that this adaptive response mechanism may allow *Mtb* to advantageously balance its growth in nutrient-limiting intracellular environments (i.e., within macrophages) in a manner that is contingent on host innate immunity.[23]

Given the nongenetically encoded nature of carbohydrates, lipids, and their conjugates, there is considerable experimental difficulty associated with investigating mycomembrane remodeling and its contributions to the complex and dynamic host–pathogen interactions that underlie *Mtb* infection. To date, such studies have mainly been restricted to the use of mutant strains along with radiolabeling and cellular fractionation techniques, a combined approach that has various experimental and practical limitations. In the past few years, the development of chemical probes has enabled tagging and analysis of various mycomembrane components in living mycobacterial cells.[24,25] Fluorescent, clickable, and radiolabeled trehalose analogues have been developed by various labs, including ours, and have permitted metabolic labeling of TMM and TDM.[26−32] We also recently developed TMM analogues that exploit Ag85 activity to label TDM, AGM, or proteins that are post-translationally modified with mycolates.[33−35] The Kiessling group recently expanded upon the TMM probe concept with a FRET-based fluorogenic TMM analogue (QTF), which generated fluorescence upon Ag85-mediated separation of its trehalose-linked quencher and lipid-linked fluorophore.[36] QTF was used to perform real-time fluorescence imaging of Ag85 activity during mycobacterial growth and division, which highlighted the complementarity of fluorogenic probes that report directly on enzyme activity as opposed to metabolically tagging the products of enzymatic reactions.[36] While significant effort has been put forth to develop probes of Ag85-catalyzed reactions and their cellular products, to date there is a lack of probes that are designed to report on TDM breakdown, which, as described above, is a critical stress-responsive mycomembrane remodeling mechanism that may be conserved across mycobacteria. Here, we describe the development of FRET-TDM, which is a synthetic fluorescence-quenched TDM analogue that fluoresces upon hydrolysis by Tdmh and potentially other mycomembrane-remodeling enzymes. Our studies demonstrate the utility and limitations of this fluorogenic probe in various assays, as well as offer insights for future optimization of probe structure and applications in mycobacteriology.

RESULTS AND DISCUSSION

Synthetic FRET-TDM Is a Fluorescence-Quenched TDM Analogue. As a first-generation fluorogenic probe for detecting TDM breakdown, we designed FRET-TDM (**1**),

DOI: 10.1021/acsomega.9b00130
ACS Omega 2019, 4, 4348−4359

Scheme 1. (A) Proposed Fluorescence-Quenched TDM Analogue, Which Is Designed To Be Activated by Tdmh (Note: Either Acyl Chain Could Be Cleaved); Star, Fluorophore; Square, Quencher; R = H or Trehalose; (B) Structure of FRET-TDM (1); (C) Synthesis of 1[a]

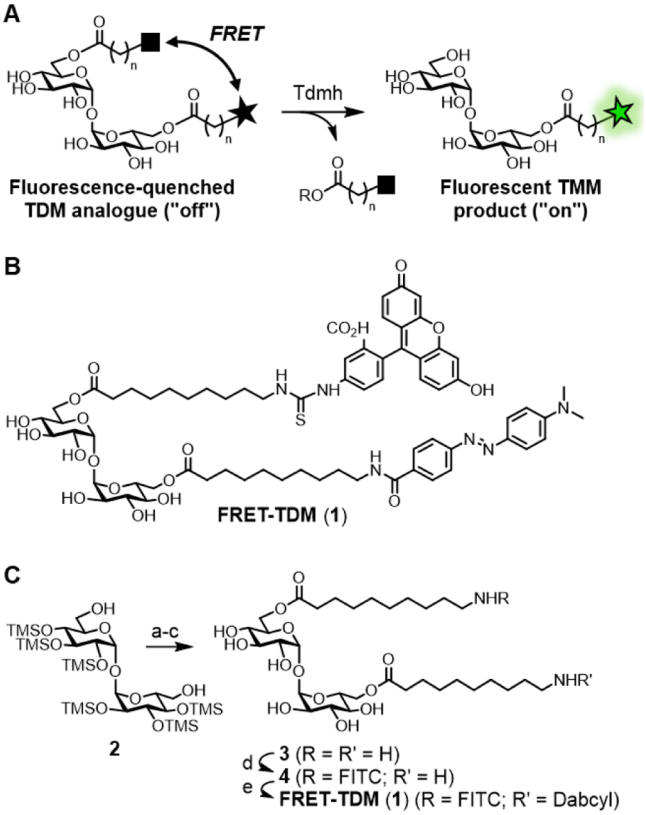

[a]Conditions: (a) DCC, DMAP, 10-Azidodecanoic Acid, CH_2Cl_2; (b) Dowex 50WX8-400 H^+ Resin, CH_3OH, 97% over two steps; (c) Pd/C, H_2, CH_2Cl_2/CH_3OH (2:1), 99%; (d) FITC, Et_3N, DMF, CH_3OH, 30%; (e) Dabcyl NHS Ester, Et_3N, CH_3OH, DMF, 81%.

which consists of a TDM-mimicking core bearing two linear 10-carbon acyl chains functionalized at their termini with fluorescein as the fluorophore and dabcyl as the quencher (Scheme 1). In a fully extended conformation, FRET-TDM's fluorophore and quencher are separated by a maximum of ∼40 Å, so we expected that these moieties were far enough away from the TDM core to allow recognition and processing by TDM-degrading hydrolases, but close enough together in the esterified state to provide efficient fluorescence quenching. Although native TDM possesses α-branched, β-hydroxyl mycolate groups (Figure 1B), we chose to install more synthetically tractable linear chains, which our prior work on TMM-based probes showed can still be tolerated by mycoloyl ester-processing enzymes.[33−35] The synthesis of FRET-TDM (Scheme 1C) was initiated by diacylation of diol **2**[37] with 10-azidodecanoic acid in the presence of dicyclohexylcarbodiimide (DCC) and 4-dimethylaminopyridine (DMAP), followed by acid-mediated desilylation and Pd-catalyzed azide reduction to give symmetrical diamine **3** in 96% yield over three steps. Diamine **3** was desymmetrized via reaction with fluorescein isothiocyanate (FITC), giving intermediate **4** in 30% yield, with the other major reaction components being unreacted **3** and the doubly FITC-modified molecule. Compound **4** was subsequently reacted with the activated NHS ester of dabcyl to deliver FRET-TDM in 81% yield following purification on a preparative C18 column. This synthetic strategy is modular, as diamine **3** can be sequentially reacted with any pair of amine-reactive fluorophore and quencher to obtain different FRET probes.

Next, we evaluated the quenching efficiency of FRET-TDM. For comparison, we synthesized one of the possible esterase-cleaved fluorescent byproducts of FRET-TDM, a fluorescein-modified TMM derivative (FITC-TMM, Scheme S1). Evaluation of concentration-dependent fluorescence of FRET-TDM and FITC-TMM in the concentration range used for biological experiments demonstrated that FRET-TDM had a quenching efficiency of 98.7% (Figure 2A). Thus, in its intact form, FRET-TDM was confirmed to be in an "off" state, which, upon enzymatic separation of the fluorophore and quencher, would be converted to a brightly fluorescent "on" state. FRET-TDM also exhibited good hydrolytic stability in various buffers and media in the absence of enzyme (Figure S1). It is notable that, in its quenched state, FRET-TDM exhibited variable background fluorescence in different types of buffers and media (Figure S1), underscoring the importance of using the same matrix for comparison of FRET-TDM activation between samples.

FRET-TDM Is Activated by Purified Mycomembrane-Remodeling Enzymes. As Tdmh and Ag85 are, in principle, both capable of breaking down mycoloyl trehalose linkages, we tested recombinant Tdmh from *M. smegmatis* and a representative Ag85 isoform, Ag85C from *Mtb*, for hydrolytic cleavage of FRET-TDM. Following optimization of probe and enzyme concentrations (Figure S2), reactions were performed with FRET-TDM (10 μM) in the presence of 10 μg/mL of purified Tdmh, Ag85C, or their corresponding inactive catalytic serine mutants $Tdmh_{S124A}$ and $Ag85C_{S124A}$ (or in buffer without enzyme). Fluorescence was monitored continuously using a plate reader (excitation/emission 485/535 nm) over 16 h. Both Tdmh and Ag85C showed time-dependent activation of the probe, with Tdmh showing faster probe turn-on than Ag85C; the catalytic mutants and buffer control showed virtually no increase in fluorescence over 16 h (Figure 2B). For both Tdmh and Ag85C, a maximum fluorescence value was reached, which then gradually dropped, possibly due to the relatively low photostability of fluorescein. At the 90 min time point, Tdmh and Ag85C treatment led to approximately 100- and 25-fold fluorescence turn-on, respectively (Figure 2C). Consistent with these results, Michaelis−Menten kinetic analysis of FRET-TDM hydrolysis by Tdmh revealed K_m and k_{cat}/K_m values of 1.99 ± 0.42 (μM) and 0.22 ± 0.05 (min^{-1} μM^{-1}), respectively, whereas for Ag85C these parameters were 0.71 ± 0.07 (μM) and 0.10 ± 0.01 (min^{-1} μM^{-1}) (Figure 2D,E). These data indicate that while Ag85C binds slightly more tightly to FRET-TDM, Tdmh catalyzes its hydrolysis more rapidly and is generally more efficient at activating the probe, as anticipated. The ability to capitalize on FRET-TDM's fluorogenic design to define the kinetic parameters of hydrolase-catalyzed probe activation will facilitate future structural optimization efforts aimed at enhancing probe specificity for mycobacterial enzymes.

Next, we used mass spectrometry (MS) to characterize the reaction products of Tdmh-catalyzed FRET-TDM breakdown. Previous work established that Tdmh catalyzes the release of free mycolic acid from TDM,[21] but to date it has not been determined whether the reaction products are TMM and one mycolic acid (as shown in Figure 1B) or trehalose and two mycolic acids. FRET-TDM was incubated in the presence or absence of Tdmh for 24 h, and then the reaction mixtures were analyzed by ESI-MS. In the no-enzyme control sample, only

DOI: 10.1021/acsomega.9b00130
ACS Omega 2019, 4, 4348−4359

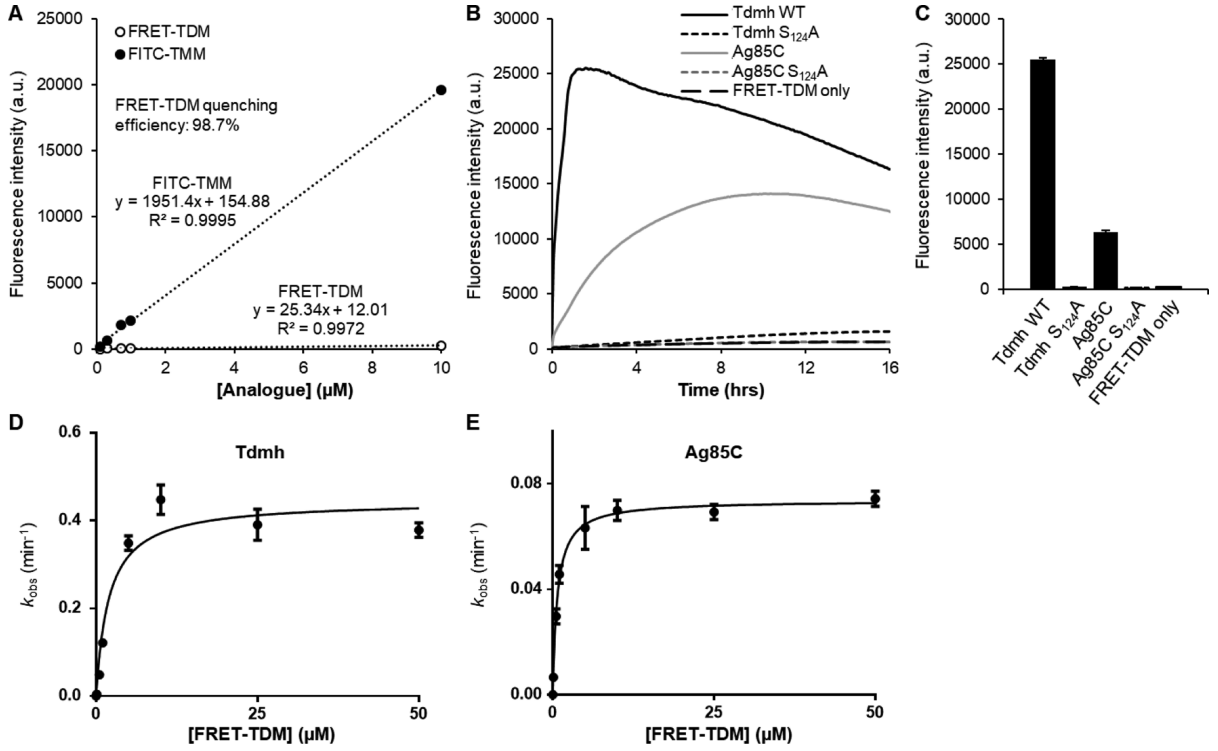

Figure 2. In vitro evaluation of FRET-TDM. (A) Quenching efficiency of intact FRET-TDM was determined by comparing the slopes of lines generated from the plot of fluorescence intensity vs concentration of "off" FRET-TDM and its "on" product FITC-TMM. (B) Plot of time-dependent fluorescence turn-on of FRET-TDM by *Msmeg* Tdmh and *Mtb* Ag85C compared to probe-only and catalytic mutant controls. (C) Bar graph of fluorescence intensities from (B) at 90 min. (D,E) Michaelis−Menten plots of k_{obs} (min^{-1}) vs the concentration of FRET-TDM for *Msmeg* Tdmh and *Mtb* Ag85C. Mean values from three replicate experiments are shown for (A−E) and error bars in (C−E) represent the standard deviation.

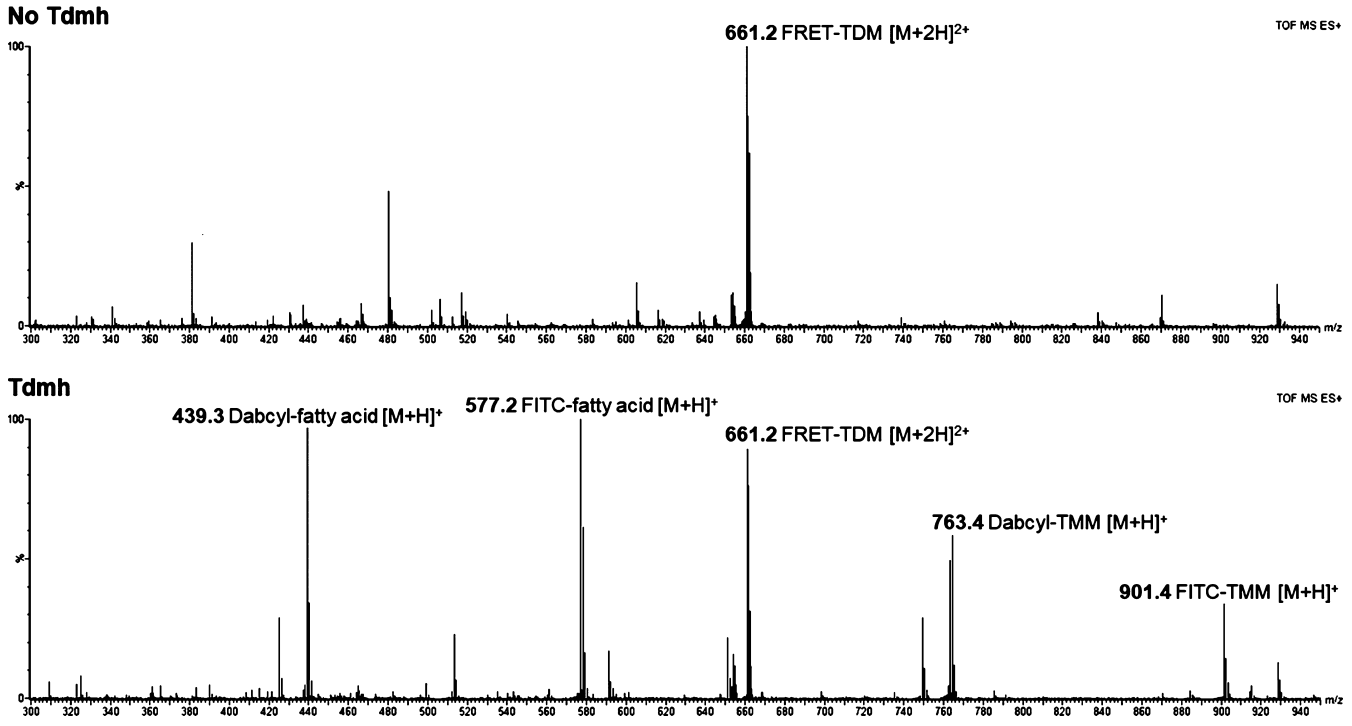

Figure 3. ESI mass spectra of FRET-TDM incubated in the absence (top) and presence (bottom) of *Msmeg* Tdmh in Tris-HCl buffer at 37 °C for 24 h. *Y*-axis, relative ion abundance.

unreacted FRET-TDM was observed, whereas in the sample exposed to Tdmh, peaks were observed for unreacted FRET-TDM and the four possible products of single-chain cleavage, including FITC- and dabcyl-modified TMM and 10-carbon fatty acid derivatives (Figure 3). These results confirmed that Tdmh indeed degrades FRET-TDM by hydrolyzing the 6-position

DOI: 10.1021/acsomega.9b00130
ACS Omega 2019, 4, 4348−4359

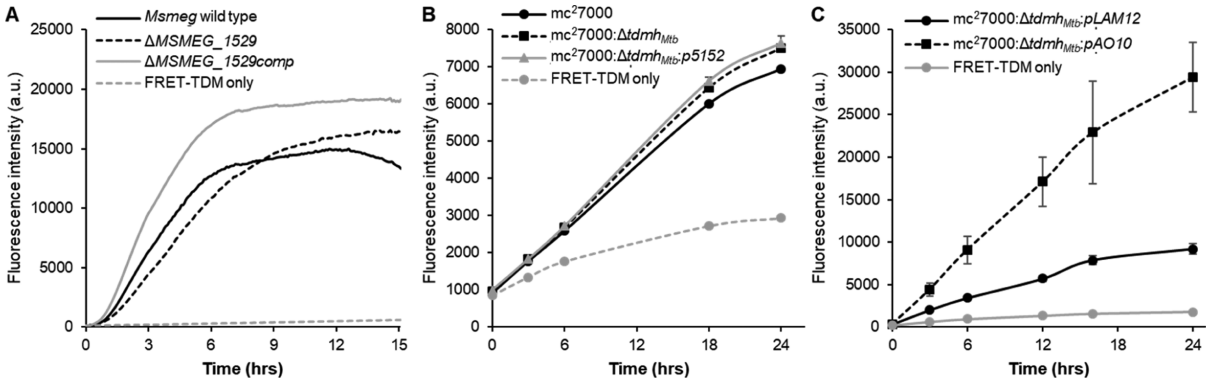

Figure 4. FRET-TDM activation by live mycobacteria. (A) Probe activation by *Msmeg* wild type, Tdmh-deficient *Msmeg* (Δ*MSMEG_1529*), and Tdmh-overexpressing *Msmeg* (Δ*MSMEG_1529comp*). (B) Probe activation by attenuated *Mtb* (mc²7000), Tdmh-deficient *Mtb* (mc²7000:Δ$tdmh_{Mtb}$), and its complement (mc²7000:Δ$tdmh_{Mtb}$:*p5152*). (C) Probe activation by a Tdmh-deficient *Mtb* strain expressing *Msmeg* Tdmh under the control of an acetamide-inducible promoter (mc²7000:Δ$tdmh_{Mtb}$:*pAO10*) and its corresponding empty plasmid control strain (mc²7000:Δ$tdmh_{Mtb}$:*pLAM12*), both in the presence of acetamide. For (A), *Msmeg* strains were cultured in the presence of FRET-TDM (10 μM) and fluorescence was monitored continuously in a plate reader over 15 h. For (B,C), *Mtb* strains were cultured in the presence of FRET-TDM (10 μM) over 24 h and fluorescence was analyzed at the time points indicated. Mean values from three replicate experiments are shown for (A−C) and error bars in (B,C) represent the standard deviation. All experiments were performed alongside a probe-only control consisting of FRET-TDM (10 μM) in the appropriate medium. See Table S1 for strain descriptions and references.

ester bonds. No obvious preference of the enzyme for hydrolyzing the FITC- or dabcyl-modified acyl chain was observed, which is not surprising given that these modifications are distant from the reaction site. Furthermore, free trehalose was not observed in the Tdmh-treated sample by ESI-MS. Assuming comparable detection efficiency for the relevant product ions, this result suggests that Tdmh produces TMM and one mycolic acid but does not further degrade TMM to trehalose, supporting the model shown in Figure 1B. Taken together, the in vitro fluorescence and MS evaluation data demonstrate that FRET-TDM is a fluorescence-quenched TDM analogue which can be used to monitor the hydrolytic activity of purified TDM-degrading hydrolases involved in mycomembrane remodeling, including Tdmh.

FRET-TDM Is Activated by Live Mycobacterial Cells. Having confirmed that FRET-TDM can be turned on by purified Tdmh, we proceeded to test whether the probe was activated by whole mycobacterial cells (see Table S1 for mycobacterial strains used in this study). First, we evaluated the kinetics of FRET-TDM activation by live *Msmeg* strains growing logarithmically, as assessed by continuous fluorescence monitoring during an overnight culture experiment (Figure 4A). Wild-type *Msmeg* mc²155 elicited rapid fluorescence turn-on and the signal plateaued at approximately 6 h with a >100-fold increase in fluorescence relative to the initial time point. To assess the contribution of Tdmh to the observed fluorescence signal, we evaluated FRET-TDM activation in a strain devoid of Tdmh (Δ*MSMEG_1529*) and in a complemented strain that overexpresses Tdmh under the control of the hsp60 promoter (Δ*MSMEG_1529comp*).[21] The fluorescence values for Δ*MSMEG_1529* tracked very closely with those from wild-type *Msmeg*, with perhaps slightly slower probe activation. Thus, although wild-type *Msmeg* triggers efficient turn-on of FRET-TDM, it occurs in a predominantly (if not completely) Tdmh-independent manner. This suggests that, under the conditions tested, physiological levels of Tdmh in *Msmeg* are too low to be detected by FRET-TDM, and thus other more abundant mycobacterial hydrolases may be responsible for the cumulative signal from probe cleavage. On the other hand, the Tdmh-overexpressing strain, Δ*MSMEG_1529comp*, activated FRET-TDM more rapidly than wild-type *Msmeg* and clearly resulted in higher overall fluorescence intensities, indicating that the probe is capable of reporting on Tdmh activity in cells if the enzyme is sufficiently abundant.

Next, we evaluated FRET-TDM activation in *Mtb* mc²7000, which is an attenuated strain of *Mtb*.[38] As with *Msmeg*, *Mtb* mc²7000 showed time-dependent FRET-TDM turn-on, registering an 8-fold enhancement in fluorescence intensity after 24 h compared to the initial time point (Figure 4B). The lower efficiency of probe activation in *Mtb* versus *Msmeg* is likely due to the former's exceptionally slow growth rate, but could also be affected by factors such as lower permeability of the probe. No changes in fluorescence were observed in an *Mtb* mc²7000 mutant lacking Tdmh (mc²7000:Δ$tdmh_{Mtb}$) or its complement (mc²7000:Δ$tdmh_{Mtb}$:*p5152*),[23] demonstrating that the signal detected in the parent strain was produced in a Tdmh-independent manner, which is consistent with the results from *Msmeg* (Figure 4A). As with *Msmeg*, we also evaluated whether overexpression of Tdmh could trigger FRET-TDM activation in *Mtb* by testing probe turn-on in a modified strain of mc²7000:Δ$tdmh_{Mtb}$ expressing *Msmeg* Tdmh under the control of an acetamide-inducible system (mc²7000:Δ$tdmh_{Mtb}$:*pAO10*) compared to its corresponding empty vector control (mc²7000:Δ$tdmh_{Mtb}$:*pLAM12*).[23] FRET-TDM was indeed activated by Tdmh-overexpressing mc²7000:Δ$tdmh_{Mtb}$:*pAO10* more efficiently than under control conditions (Figure 4C). This result, which is consistent with the data from *Msmeg*, suggests that FRET-TDM is capable of reporting on Tdmh activity in live *Mtb* cells if the enzyme activity is induced.

Our results in *Msmeg* and *Mtb* suggest that basal levels of Tdmh are too low to be detected by FRET-TDM, but that the probe may detect Tdmh when its expression is elevated (e.g., through genetic overexpression, as shown above). Because Tdmh-mediated mycomembrane remodeling is reportedly induced under nutrient-limiting conditions,[21,23] we hypothesized that cell starvation would induce Tdmh expression, leading to Tdmh-dependent FRET-TDM activation. To test this hypothesis, *Msmeg* or *Mtb* strains were incubated in either nutrient-rich medium or starvation conditions (PBS) and FRET-TDM activation was assessed. Regardless of whether FRET-

DOI: 10.1021/acsomega.9b00130
ACS Omega 2019, 4, 4348−4359

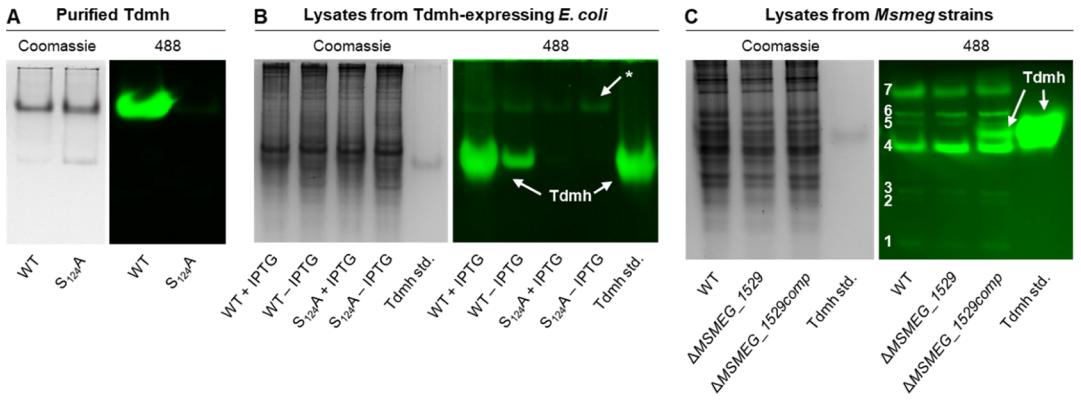

Figure 5. FRET-TDM activation by purified Tdmh and bacterial cell lysates using a native PAGE fluorescence assay. Proteins or lysates were resolved by native PAGE in parallel gels, one of which was Coomassie-stained (left) and the other was soaked in FRET-TDM (10 μM) and scanned for fluorescence (right). (A) Analysis of purified Tdmh and $Tdmh_{S124A}$ (1.5 μg loaded into each lane). (B) Analysis of lysates from induced (+IPTG) or uninduced (−IPTG) Tdmh- or $Tdmh_{S124A}$-expressing *E. coli*. The asterisk (*) marks a non-Tdmh band present in *E. coli* lysate. (C) Analysis of lysates from *Msmeg* wild type, Tdmh-deficient (Δ*MSMEG_1529*), or Tdmh-overexpressing (Δ*MSMEG_1529comp*) strains. The arrows mark Tdmh and 1−7 mark bands fluorescing in all *Msmeg* lysates.

TDM was added to cells at the onset of PBS starvation or after a period of up to 4 days of starvation, we did not observe Tdmh-dependent probe turn-on in *Msmeg* or *Mtb* (Figures S3 and S4). The efficiency of FRET-TDM activation was also significantly lower in starved cells. Thus, at least under the culture conditions tested and the assay used here, FRET-TDM did not report on physiologically relevant Tdmh activity in whole mycobacterial cells. This result is probably due to the low abundance of Tdmh in cells, which has been noted in earlier reports. Prior work showed that when recombinant Tdmh was exogenously added to cells, TDM was degraded to the point of cell lysis, implying that mycobacteria must tightly regulate the concentration of active Tdmh to avoid autolysis while also allowing for beneficial mycomembrane remodeling to occur.[22] Consistent with this explanation and with our data, Yang et al. previously reported that physiological levels of Tdmh could not be directly detected by western blot using an anti-Tdmh antibody, supporting the conclusion that Tdmh is a low-abundance enzyme.[23] Overall, while FRET-TDM is an excellent fluorogenic reporter of Tdmh activity in vitro and it is capable of reporting on Tdmh activity in vivo, the probe may have a limited capacity at its current level of sensitivity to monitor mycomembrane remodeling mediated by low-abundance levels of Tdmh in live cells.

Native PAGE Fluorescence Assay Reveals Multiple FRET-TDM-Activating Enzymes in Mycobacteria. We were intrigued that FRET-TDM was activated by *Msmeg* and *Mtb* cells in a Tdmh-independent manner, which implied that other enzymes were cleaving the probe and thus may be candidate mycomembrane-remodeling enzymes. To test this possibility, we established a native polyacrylamide gel electrophoresis (PAGE)-based hydrolase profiling assay that capitalized on the fluorogenic design of FRET-TDM. This assay, which was inspired by prior work deploying other fluorogenic esterase probes in mycobacteria,[39,40] involved the separation of protein samples (either purified proteins or cell lysates) on a native polyacrylamide gel to retain their activity, then bathing the gel in FRET-TDM and performing in-gel fluorescence scanning to detect FRET-TDM-degrading enzymes. To verify the assay, we first evaluated purified Tdmh and its active site mutant $Tdmh_{S124A}$. In agreement with the data shown in Figure 2B,C, wild-type Tdmh generated a strong fluorescence band, whereas the mutant enzyme did not produce fluorescence (Figure 5A).

Next, we tested whether the assay could specifically detect Tdmh activity in more complex cell lysate samples. *Escherichia coli* strains[21,22] engineered to produce either wild-type Tdmh or its catalytic mutant $Tdmh_{S124A}$ were induced to express these proteins by treatment with isopropyl β-D-1-thiogalactopyranoside (IPTG), or left unexposed to IPTG as controls, then lysates were collected. Analysis of the *E. coli* cell lysates using the FRET-TDM native gel assay showed a major fluorescence band corresponding to Tdmh in the IPTG-treated sample and a minor Tdmh band in the IPTG-untreated control, the latter likely due to leaky expression (Figure 5B). For the $Tdmh_{S124A}$ mutant samples, no fluorescence signal was detected in the Tdmh migration area. The specificity of FRET-TDM for Tdmh activity in an *E. coli* lysate background was exceptional, as only a single faint band was observed that appeared to be a non-Tdmh protein endogenous to *E. coli* (band marked with an asterisk in Figure 5B). These experiments showed that FRET-TDM can be coupled with native PAGE to detect TDM-hydrolyzing enzymes in complex cell lysates.

Next, we applied the native gel fluorescence assay to profile FRET-TDM-activating proteins in cell lysates obtained from *Msmeg* strains, including the aforementioned Tdmh mutant (Δ*MSMEG_1529*) and overexpression (Δ*MSMEG_1529comp*) strains (Figure 5C). The wild-type *Msmeg* sample (lane 1) showed several fluorescent bands (marked as bands 1−7), including one dominant band (marked as band 4), but none appearing to co-migrate with a purified standard of Tdmh (lane 4). The mutant banding pattern (lane 2) was identical to the wild type, whereas the Tdmh-overexpressing strain Δ*MSMEG_1529-comp* (lane 3) clearly revealed a new band co-migrating with Tdmh (marked with an arrow). Lysates from *Msmeg* starved in PBS did not exhibit a detectable Tdmh band (data not shown). Together, these results mirrored our observations from the cell assays, namely that: (i) FRET-TDM can detect Tdmh activity if the protein level is sufficient; and (ii) other mycobacterial enzymes with hydrolase activity likely have significant contribution to probe activation. A likely candidate is Ag85C or other Ag85 isoforms, which are abundant in mycobacteria and therefore may produce a strong signal despite weaker activity relative to Tdmh (Figure 2). The identities of the unknown bands observed in the mycobacterial lysates (Figure 5C, lane 1) are of high interest, as they could possibly include novel

DOI: 10.1021/acsomega.9b00130
ACS Omega 2019, 4, 4348−4359

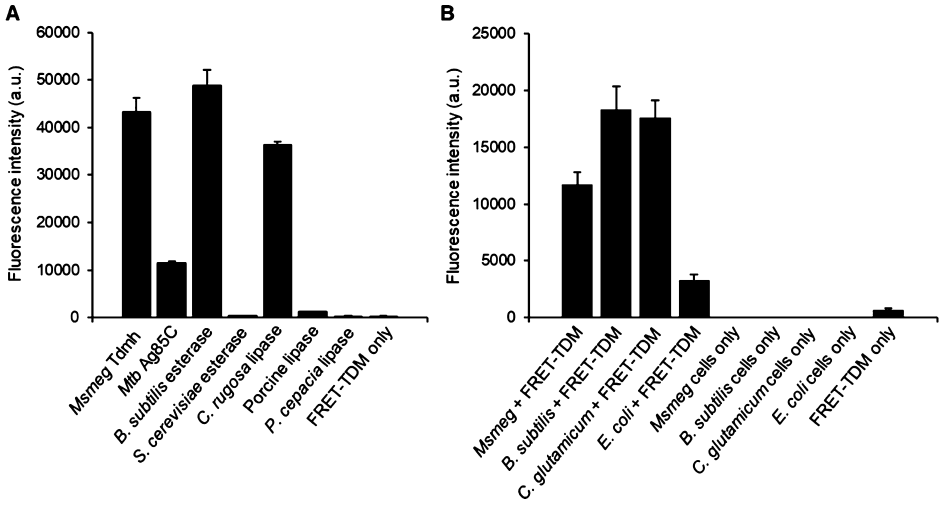

Figure 6. FRET-TDM activation by panels of hydrolases and bacteria. FRET-TDM (10 μM) was incubated in the presence of (A) 10 μg/mL of hydrolases from various sources or (B) different types of bacteria. Mean values from three replicate experiments are shown and error bars represent the standard deviation. See Figures S5 and S6 for time-dependent fluorescence activation.

hydrolases involved in mycomembrane remodeling. FRET-TDM coupled with native PAGE can potentially be used as a tool to facilitate the identification and characterization of these types of enzymes. Future work in this area will focus on combining FRET-TDM assays with MS, genetic, and biochemical techniques to elucidate the identities and functions of these candidate mycomembrane-remodeling enzymes.

FRET-TDM Exhibits Partial Selectivity for Mycobacterial Hydrolases. Fluorogenic probes that target mycobacteria-specific pathways could eventually aid in the diagnosis of tuberculosis and related diseases by improving the detection of pathogenic mycobacteria (e.g., *Mtb*) in patient samples.[30,41] Fluorescence-quenched TDM analogues are a new entry into this probe category, so we sought to evaluate their selectivity for mycobacterial enzymes. The low background fluorescence of FRET-TDM in *E. coli* lysates was a preliminary indication of its selectivity (Figure 5B). To further investigate FRET-TDM's selectivity, we tested its activation by purified Tdmh, Ag85C, and a panel of commercially available hydrolases, which included several prokaryotic and eukaryotic esterases and lipases (all tested at 10 μg/mL enzyme concentration). The relative efficiency of probe turn-on by Tdmh and Ag85C was the same as our prior experiments (Figure 2B,C), while mixed results were obtained from the other enzymes (Figure 6A; see Figure S5 for fluorescence intensities plotted vs time). While hydrolases from yeast, porcine, and *Pseudomonas cepacia* showed virtually no increase in fluorescence versus the probe-only control, *Bacillus subtilis* esterase and *Candida rugosa* lipase activated FRET-TDM with approximately the same efficiency as Tdmh. Next, we tested the selectivity of FRET-TDM activation by whole cells of different bacterial types, including *Msmeg* and the related organism *Corynebacterium glutamicum*, which also has a mycomembrane-like outer membrane that is rich in TDM,[42] as well as *E. coli* and *B. subtilis*, which are representative Gram-negative and Gram-positive bacteria, respectively. Logarithmically growing cells of each species were washed, normalized to the same density, re-suspended in PBS with FRET-TDM, and incubated at 37 °C while monitoring fluorescence over approximately 14 h. All four types of bacteria activated the probe, with *B. subtilis* and *C. glutamicum* giving the highest fluorescence, followed by *Msmeg* and then *E. coli* (Figure 6B; see Figure S6 for fluorescence intensities plotted vs time).

Taken together, these results show that although FRET-TDM is activated by mycobacterial Tdmh and Ag85, which act on trehalose mycoloyl esters, some non-mycobacterial hydrolases and cell types also turn on the probe. Thus, the probe design, which is based on a trehalose diester scaffold that occurs almost exclusively in the Corynebacterineae suborder, does confer a measure of mycobacterial selectivity to FRET-TDM, but only partially so. Perhaps replacing the naturally occurring α-branched, β-hydroxylated mycolate groups of TDM with more synthetically accessible linear chains rendered FRET-TDM's ester linkages susceptible to cleavage by a broader range of hydrolases. Native mycolates feature an unusual amount of steric bulk and a secondary hydroxyl group near the ester bond (see Figure 1B), which, if present in FRET-TDM, may deter much of the observed nonspecific probe activation. For instance, recent work by Goins et al. suggested that the β-hydroxyl group of mycolates plays an important role in Ag85 catalysis.[43] Thus, the first-generation FRET-TDM probe reported here needs to be optimized to improve: (i) its specificity for TDM-related metabolic pathways and (ii) its ability to discriminate mycobacteria from other cell types. Optimization of the FRET-TDM structure should initially focus on the inclusion of acyl chains that more closely resemble native mycolates. Previously reported trehalose ester-based probes—including our clickable TMM analogues[33−35] and the Kiessling group's FRET-based TMM probe QTF[36]—also contain simplified linear acyl chains, which may present comparable specificity challenges that could be similarly addressed for improved mycobacterial detection. In the meantime, the limited specificity of FRET-TDM can be exploited to identify and facilitate the characterization of novel enzymes, which may also be involved in mycomembrane remodeling, as noted above.

CONCLUSIONS

In summary, we chemically synthesized and performed in vitro and in vivo evaluation of FRET-TDM, which is a fluorescence-quenched analogue of the virulence-associated mycomembrane glycolipid TDM. In designing the probe, we exploited the FRET phenomenon by placing the large fluorophore and quencher

DOI: 10.1021/acsomega.9b00130
ACS Omega 2019, 4, 4348−4359

groups at the ends of the linear mycolate-mimicking acyl chains—putting them in close enough proximity to each other to allow for efficient fluorescence quenching while still being distal from the ester linkages, so as not to interfere with enzymatic cleavage. The success of this design was borne out by in vitro evaluation experiments, which demonstrated that FRET-TDM, while non-fluorescent in the absence of enzyme, was efficiently activated by the mycobacteria-specific enzyme Tdmh, which is a TDM hydrolase known to be involved in stress-induced mycomembrane remodeling. FRET-TDM was also efficiently activated in the presence of whole cells of *Msmeg* and the global pathogen *Mtb*. The fact that the prevailing mechanism of probe turn-on in vivo was Tdmh-independent is consistent with the low physiological levels of this enzyme in mycobacteria. This Tdmh-independent behavior of FRET-TDM in cells led us to develop a native gel fluorescence assay to allow profiling of FRET-TDM-activating enzymes in whole-cell lysates. Several such proteins were detected in *Msmeg* lysates, revealing a number of candidate hydrolases to be further characterized in future studies. It is expected that this native gel assay, which enlists FRET-TDM as a key tool, will be valuable for elucidating mycomembrane-remodeling processes in mycobacteria and other members of the Corynebacterineae suborder. Although FRET-TDM was designed to target a mycobacteria-specific pathway, our data suggest that—in its current form—the probe has only partial selectivity for mycobacterial enzymes and cells. Structural optimization efforts emphasizing the inclusion of more-native acyl chains and improved FRET pairs into next-generation FRET-TDM (and related FRET probes) are currently underway in our lab. Building on our prior work, this study further underscores that trehalose ester-based probes, which target mycobacterial pathways that are distinct from those targeted by trehalose-based probes, are emerging as a complementary class of tools for studying and targeting mycobacteria. The latest additions to the trehalose- and trehalose ester-based probe toolbox include a solvatochromic trehalose probe (DMNTre) by the Bertozzi group,[30] a FRET-based TMM probe (QTF) by the Kiessling group,[36] and the FRET-based TDM probe (FRET-TDM) described herein. Together, these recent studies represent a shift toward probe molecules that feature no-wash, real-time fluorescence turn-on resulting from mycobacteria-specific metabolic events. Given the value of such probes for investigating cell envelope metabolism and their potential to aid in the rapid diagnosis of tuberculosis or other mycobacterial diseases, continued research to improve and expand upon these molecules is of interest.

EXPERIMENTAL SECTION

General Methods for Synthesis. Materials and reagents were obtained from commercial sources without further purification unless otherwise noted. Anhydrous solvents were obtained either commercially or from an alumina column solvent purification system. All reactions were carried out in oven-dried glassware under inert gas unless otherwise noted. Analytical thin-film chromatography (TLC) was performed on glass-backed silica gel 60 Å plates (thickness 250 μm) and detected by charring with 5% H_2SO_4 in EtOH. Column chromatography was performed using flash-grade silica gel 32−63 μm (230−400 mesh). ^{1}H NMR spectra were recorded at 500 MHz with chemical shifts in ppm (δ) referenced to solvent peaks. ^{13}C NMR spectra were recorded at 125 MHz. NMR spectra were obtained on a Varian Inova 500 instrument. Coupling constants (J) are reported in hertz (Hz). High-resolution electrospray ionization (HR ESI) mass spectra were obtained using a Waters LCT Premier XE using either raffinose or reserpine as the lock mass.

Di-6,6′-*O*-(10-azidodecanoyl)-*α*,*α*-D-trehalose. An oven-dried round-bottom flask was charged with DCC (1.900 g, 9.209 mmol) and DMAP (0.190 g, 1.555 mmol). After drying the reagents under high vacuum and placing the flask under a nitrogen atmosphere, anhydrous CH_2Cl_2 (15 mL) was added. To the stirring solution was added 10-azidodecanoic acid (1.900 g, 8.908 mmol), followed by slow, dropwise addition of a freshly prepared solution of 2,3,4,2′,3′,4′-hexakis-*O*-(trimethylsilyl)-*α*,*α*-trehalose[37] (**2**, 1.00 g, 1.29 mmol) in anhydrous CH_2Cl_2 (15 mL). After 24 h, TLC (hexanes/ethyl acetate 5:1) showed generation of the diester product (R_f = 0.65). The reaction was quenched by addition of excess CH_3OH and concentrated by rotary evaporation. After resuspension of the crude product in CH_2Cl_2, the insoluble byproduct DCU was removed by filtration. The filtrate containing crude product was concentrated by rotary evaporation and purified by silica gel chromatography (hexanes/ethyl acetate 8:1 containing 1% Et_3N) to give the diester intermediate. The intermediate was dissolved in anhydrous CH_3OH (80 mL) and placed under a nitrogen atmosphere. Dowex 50WX8-400 H^+ ion-exchange resin was added and the reaction was stirred for 1 h at room temperature, after which TLC (CH_2Cl_2/CH_3OH 5:1) indicated that the reaction was complete (R_f = 0.51). After the ion-exchange resin was filtered off, the filtrates were concentrated by rotary evaporation and filtered to give di-6,6′-*O*-(10-azidodecanoyl)-*α*,*α*-D-trehalose (0.960 g, 97% over two steps) as a white solid. ^{1}H NMR (500 MHz, CD_3OD): δ 4.95 (d, J = 4.0 Hz, 2H, H-1), 4.26 (dd, J = 2.0, 12 Hz, 2H, H-6a or 6b), 4.11 (dd, J = 5.0, 12 Hz, H-6a or 6b), 3.91 (ddd, J = 1.5, 5.0, 9.5 Hz, 2H, H-5), 3.68 (t, J = 10 Hz, 2H, H-3), 3.37 (dd, J = 3.5, 9.5 Hz, 2H, H-2), 3.23 (t, J = 10.5 Hz, 2H, H-4), 3.18 (t, J = 6.5 Hz, 4H, CH_2−N_3), 2.25 (t, J = 7.5 Hz, 4H, α-CH_2), 1.54−1.46 (m, 8H, CH_2s), 1.30−1.23 (m, 20H, CH_2s). ^{13}C NMR (125 MHz, CD_3OD): δ 175.4, 95.2, 74.5, 73.1, 71.9, 71.5, 64.4, 52.4, 35.0, 30.4, 30.2, 30.1, 29.9, 27.8, 26.0. ESI MS negative mode: calcd for $C_{19}H_{29}O_{12}$ $[M-H]^-$ m/z, 731.38; found, 731.33.

Di-6,6′-*O*-(10-aminodecanoyl)-*α*,*α*-D-trehalose (3). To a solution of di-6,6′-*O*-(10-azidodecanoyl)-*α*,*α*-D-trehalose (150 mg, 0.205 mmol) in CH_2Cl_2/CH_3OH (2:1, 6 mL) under an argon atmosphere was added Pd/C (15 mg). A hydrogen-filled balloon was connected to the reaction flask and the argon atmosphere was exchanged for hydrogen. After stirring under a hydrogen atmosphere at room temperature overnight, the reaction mixture was filtered through celite and the filtrate was concentrated by rotary evaporation to give the reduced product **3** (139 mg, 99%) as a white solid. ^{1}H NMR (500 MHz, CD_3OD): δ 4.94 (d, J = 4.0 Hz, 2H, H-1), 4.26 (dd, J = 2.5, 12.5 Hz, 2H, H-6a or H-6b), 4.11 (dd, J = 5.5, 11.5 Hz, 2H, H-6a or H-6b), 3.92 (ddd, J = 2.0, 5.5, 10.5 Hz, 2H, H-5), 3.69 (t, J = 9.5 Hz, 2H, H-3), 3.36 (dd, J = 3.5, 9.5 Hz, 2H, H-2), 3.24 (t, J = 10 Hz, 2H, H-4), 2.82 (t, J = 7.5 Hz, 4H, CH_2−NH_2), 2.26 (t, J = 7.0 Hz, 4H, α-CH_2), 1.58−1.51 (m, 8H, CH_2s), 1.33−1.22 (m, 20H, CH_2s). ^{13}C NMR (125 MHz, CD_3OD): δ 174.42, 95.30, 74.51, 73.15, 71.89, 71.49, 64.35, 40.77, 35.00, 30.24, 30.21, 30.11, 30.09, 28.55, 27.39, 26.00. HR ESI MS positive mode: calcd for $C_{32}H_{61}NO_{13}$ $[M+H]^+$, 681.4174; found, 681.4171.

6-*O*-(10-Aminodecanoyl)-6′-*O*-(10-[(fluorescein-5-yl)-thioureido]decanoyl)-*α*,*α*-D-trehalose (4). To a solution of compound **2** (30 mg, 0.044 mmol) stirring in CH_3OH (1 mL) was added a solution of FITC (17 mg, 0.044 mmol) and Et_3N (8 μL, 0.08 mmol) dissolved in *N*,*N*-dimethylformamide (DMF)

DOI: 10.1021/acsomega.9b00130
ACS Omega 2019, 4, 4348−4359

(4 mL). After stirring for 6 h, TLC (*n*-BuOH/EtOH/H_2O, 5:3:2) showed optimal conversion of **3** to **4**. The reaction mixture was concentrated by rotary evaporation and purified using a Biotage Isolera One automated flash chromatography system (2 × 10 g C18 columns in sequence; 30% CH_3CN in H_2O → 70% CH_3CN in H_2O) to give product **4** (14 mg, 30%) as a yellow solid. ^{1}H NMR (500 MHz, CD_3OD): δ 8.11 (s, broad, 1H), 7.69 (d, J = 8.5 Hz, 1H), 7.08 (d, J = 8.0 Hz, 1H), 6.67−6.59 (m, 4H), 6.49 (d, J = 7.5 Hz, 2H), 4.96 (d, J = 4.0 Hz, 2H, H-1 and H-1′), 4.27 (dd, J = 2.5, 11.5 Hz, 2H, H-6a or H-6b and H-6a′ or H-6b′), 4.11 (dd, J = 5.5, 11.5 Hz, 2H, H-6a or H-6b and H-6a′ or H-6b′), 3.94−3.91 (m, 2H, H-5 and H-5′), 3.70 (t, J = 9.5 Hz, 2H, H-3 and H-3′), 3.56−3.49 (m, 2H, CH_2−NH−fluoresceinyl), 3.40−3.37 (m, 2H, H-2 and H-2′), 3.26−3.22 (m, 2H, H-4 and H-4′), 2.89−2.81 (m, 2H, CH_2−NH_2), 2.27−2.23 (m, 4H, α-CH_2s), 1.60−1.48 (m, 8H, CH_2s), 1.33−1.19 (m, 20H, CH_2s). ^{13}C NMR (125 MHz, CD_3OD): δ 182.70, 175.44, 173.88, 171.23, 161.95, 154.39, 144.28, 142.67, 130.47, 129.02, 125.80, 113.87, 111.74, 103.49, 95.17, 74.52, 73.14, 71.88, 71.48, 64.37, 46.16, 40.77, 35.08, 35.00, 30.42, 30.34, 30.26, 30.23, 30.10, 30.08, 30.07, 29.90, 28.54, 27.97, 27.56, 27.50, 27.36, 26.05, 25.98. HR ESI MS positive mode: m/z calcd for $C_{53}H_{71}N_3O_{18}S$ $[M + 2H]^{2+}$, 535.7305; found, 535.7337.

6-*O*-(10-Aminodecanoyl)-6′-*O*-(10-[(fluorescein-5-yl)-thioureido]decanoyl)-α,α-D-trehalose (1, FRET-TDM). To a solution compound **3** (10 mg, 0.009 mmol) stirring in CH_3OH (0.5 mL) was added a solution of dabcyl NHS ester (3 mg, 0.009 mmol) and Et_3N (4 μL, 0.03 mmol) dissolved in DMF (2 mL). After stirring for 5 h, TLC (*n*-BuOH/EtOH/H_2O, 5:3:2) showed complete consumption of **4**. The reaction mixture was concentrated by rotary evaporation and purified using a Biotage Isolera One automated flash chromatography system (2 × 10 g C18 columns in sequence; 30% CH_3CN in H_2O → 70% CH_3CN in H_2O) to give product **1** (10 mg, 81%) as an orange-yellow solid. ^{1}H NMR (500 MHz, CD_3OD containing 10% $CDCl_3$): δ 8.21 (s, broad, 1H), 8.06−7.96 (m, 7H), 7.27 (d, J = 8.0 Hz, 1H), 6.96−6.90 (m, 4H), 6.83 (s, broad, 2H), 6.70 (d, J = 8.0 Hz, 2H), 5.23 (d, J = 4.0 Hz, 2H, H-1 and H-1′), 4.48 (dd, J = 2.0, 11.5 Hz, 2H, H-6a or H-6b and H-6a′ or H-6b′), 4.40 (dd, J = 5.5, 12.5 Hz, 2H, H-6a or H-6b and H-6a′ or H-6b′), 4.15−4.09 (m, 2H, H-5 and H-5′), 3.91 (t, J = 8.5 Hz, 2H, H-3 and H-3′), 3.84−3.87 (m, 2H, CH_2−NH−fluoresceinyl), 3.68−3.63 (m, 2H, H-2 and H-2′), 3.56−3.50 (m, 4H, H-4, H-4′, and CH_2−NH-dabcyl), 3.26 (s, 6H, dabcyl CH_3s), 2.48 (t, J = 7.5 Hz, 4H, α-CH_2s), 1.86−1.79 (m, 8H, CH_2s), 1.58−149 (m, 20H, CH_2s). ^{13}C NMR (125 MHz, CD_3OD containing 10% $CDCl_3$): δ 175.07, 170.83, 168.82, 162.31, 157.84, 155.45, 154.02, 153.60, 144.07, 143.94, 135.16, 132.03, 130.00, 128.52, 125.04, 122.77, 122.43, 111.99, 103.24, 94.14, 73.82, 72.21, 70.91, 63.72, 45.12, 40.67, 40.44, 30.10, 29.84, 29.79, 29.73, 29.68, 29.63, 29.58, 29.48, 29.46, 29.26, 27.47, 27.35, 26.09, 25.29. ESI MS positive mode: m/z calcd for $C_{68}H_{86}N_6O_{19}S$ $[M + 2H]^{2+}$, 661.2834; found, 661.2787.

6-*O*-(10-Azidodecanoyl)-α,α-D-trehalose (See Scheme S1). An oven-dried round-bottom flask was charged with DCC (107 mg, 0.52 mmol) and DMAP (0.236 g, 1.94 mmol). After drying the reagents under high vacuum and placing the flask under a nitrogen atmosphere, anhydrous CH_2Cl_2 (2 mL) was added and the mixture was cooled to 0 °C. To the stirring solution was added 10-azidodecanoic acid (55 mg, 0.258 mmol), followed by slow, dropwise addition of a freshly prepared solution of 2,3,4,2′,3′,4′-hexakis-*O*-(trimethylsilyl)-α,α-trehalose[37] (**2**, 0.200 g, 0.258 mmol) in anhydrous CH_2Cl_2 (2 mL). The reaction mixture was stirred and gradually allowed to warm to room temperature. After TLC (hexanes/ethyl acetate 4:1) showed generation of the monoester as the major product (approximately 4 h), the reaction was quenched by addition of excess CH_3OH and concentrated by rotary evaporation. After resuspension of the crude product in CH_2Cl_2, the insoluble byproduct DCU was removed by filtration. The filtrate containing crude product was concentrated by rotary evaporation and purified by silica gel chromatography (hexanes/ethyl acetate containing 1% Et_3N) to give the monoester intermediate as a pale yellow syrup. The intermediate was dissolved in a mixture of anhydrous CH_3OH (12 mL) and anhydrous CH_2Cl_2 (5 mL) and placed under a nitrogen atmosphere. Dowex 50WX8-400 H^+ ion-exchange resin was added and the reaction was stirred for 30 min at room temperature, after which TLC (CH_2Cl_2/CH_3OH 2:1) indicated that the reaction was complete. After the ion-exchange resin was filtered off, the filtrates were concentrated by rotary evaporation and filtered to give 6-*O*-(10-azidodecanoyl)-α,α-D-trehalose (48 mg, 44% over two steps). ^{1}H NMR (500 MHz, CD_3OD): δ 5.01 (d, J = 3.5 Hz, 1H, H-1′), 4.99 (d, J = 3.5 Hz, 1H, H-1), 4.30 (dd, J = 2.0, 12 Hz, 1H, H-6a′ or 6b′), 4.12 (dd, J = 5.0, 11.5 Hz, 1H, H-6a′ or 6b′), 3.94 (ddd, J = 2.0, 5.0, 10 Hz, 1H, H-5′), 3.77−3.67 (m, 4H, H-3, 3′, 5, 6a or 6b), 3.64 (dd, J = 5.0, 7.0 Hz, 1H, H-6a or 6b), 3.40−3.37 (m, 2H, H-2, 2′), 3.27−3.22 (m, 2H, H-4, 4′), 3.19 (t, J = 7.0 Hz, 2H, CH_2−N_3), 2.31 (t, J = 7.0 Hz, 2H, α-CH_2), 1.55−1.47 (m, 4H, CH_2s), 1.31−1.22 (m, 10H, CH_2s). ^{13}C NMR (125 MHz, CD_3OD): δ 175.4, 95.2, 95.1, 74.6, 74.4, 73.9, 73.2, 73.1, 71.9, 71.8, 71.4, 64.4, 62.6, 52.4, 35.0, 30.5, 30.3, 30.2, 30.1, 29.9, 27.8, 26.0. HR ESI MS negative mode: calcd for $C_{23}H_{40}N_3O_{14}$ $[M + CHO_2^-]^-$, 582.2510; found, 582.2529.

6-*O*-(10-Aminodecanoyl)-α,α-D-trehalose (5, See Scheme S1). To a solution of compound 6-*O*-(10-azidodecanoyl)-α,α-D-trehalose (51 mg, 0.095 mmol) in CH_2Cl_2/CH_3OH (2:1) under an argon atmosphere was added Pd/C (35 mg). A hydrogen-filled balloon was connected to the reaction flask and the argon atmosphere was exchanged for hydrogen. After stirring under a hydrogen atmosphere at room temperature overnight, the reaction mixture was filtered through celite and the filtrate was concentrated by rotary evaporation to give the reduced product **5** (48 mg, 99%) as a white solid. ^{1}H NMR (500 MHz, D_2O): δ 5.16 (d, J = 4.0 Hz, 1H, H-1′), δ 5.14 (d, J = 4.0 Hz, 1H, H-1), 4.42 (dd, J = 2.0, 12 Hz, 1H, H-6′a or b), δ 4.30 (dd, J = 5.0, 12 Hz, 1H, H-6′a or b), 4.01 (ddd, J = 2.0, 5.0, 10 Hz, 1H, H-5′), 3.86−3.78 (m, 4H, H-3′, 3, 5, 6a or 6b), 3.74 (dd, J = 5.0, 12 Hz, 1H, H6a or b), 3.63 (dd, J = 4.0, 9.5 Hz, 1H, H-2′), 3.61 (dd, J = 4.0, 10 Hz, 1H, H-2), 3.48 (t, J = 10 Hz, 1H, H-4′), 3.42 (t, J = 10 Hz, 1H, H-4), 2.97 (t, J = 8.0 Hz, 2H, CH_2−NH_2), 2.42 (t, J = 7.5 Hz, 2H, α-CH_2), 1.67−1.59 (m, 4H, CH_2s), 1.38−1.26 (m, 10H, CH_2s). ^{13}C NMR (125 MHz, D_2O): 177.9, 94.7, 94.6, 73.9, 73.7, 73.5, 72.4, 72.3, 71.3, 71.1, 71.0, 64.3, 61.9, 40.8, 35.1, 29.7, 29.6, 29.5, 29.4, 28.0, 26.9, 25.6. HR ESI MS positive mode: calcd for $C_{22}H_{42}NO_{12}$ $[M + H]^+$, 512.2707; found, 512.2699.

6-*O*-(10-[(Fluorescein-5-yl)thioureido]decanoyl)-α,α-D-trehalose (FITC-TMM, 6, See Scheme S1). To a 20 mL glass scintillation vial containing compound **5** (15.7 mg, 0.0306 mmol) stirring in CH_3OH (0.5 mL) was added a solution of FITC (12.4 mg, 0.0316 mmol) and Et_3N (7 μL, 0.05 mmol) dissolved in *N*,*N*-DMF (1.5 mL). After stirring for 20 h, the reaction mixture was concentrated by rotary evaporation and purified using a Biotage Isolera One automated flash chromatography system (10 g C18 column; 30% CH_3CN in H_2O → 70% CH_3CN in H_2O) to give FITC-TMM (compound

DOI: 10.1021/acsomega.9b00130
ACS Omega 2019, 4, 4348−4359

6, 23.4 mg, 85%) as a yellow solid. ^{1}H NMR (500 MHz, 10% $CDCl_3$ in CD_3OD): δ 8.18 (s, broad, 1H, FITC Ar-CH), 7.86 (dd, J = 2.0, 8.5 Hz, 1H, FITC Ar-CH), 7.16 (d, J = 8.5 Hz, 1H, FITC Ar-CH), 6.71−6.69 (m, 4H, FITC Ar-CH), 6.56 (dd, J = 2.5, 9.0 Hz, 2H, FITC Ar-CH), 5.14 (d, J = 4.0 Hz, 1H, H-1′), 5.11 (d, J = 3.5 Hz, 1H, H-1), 4.38 (dd, J = 2.0, 12 Hz, 1H, H-6a′ or 6b′), 4.26 (dd, J = 5.5, 12.5 Hz, 1H, H-6a′ or 6b′), 4.03 (ddd, J = 2.0, 4.5, 10 Hz, 1H, H-5′), 3.85−3.78 (m, 4H, H-3, 3′, 5, 6a or 6b), 3.71 (dd, J = 6.0, 12 Hz, 1H, H-6a or 6b), 3.67−3.60 (m, 2H, CH_2−N), 3.55 (dd, J = 3.5, 10 Hz, 1H, H-2′), 3.51 (dd, J = 4.0, 10 Hz, 1H, H-2), 3.42−3.36 (m, 2H, H-4, 4′), 2.37 (t, J = 7.5 Hz, 2H, α-CH_2), 1.70−1.63 (m, 4H, CH_2s), 1.44−1.30 (m, 10H, CH_2s). ^{13}C NMR (125 MHz, CD_3OD): δ 181.2, 175.2, 173.4, 170.9, 153.8, 142.0, 130.0, 113.4, 111.1, 103.3, 94.6, 94.5, 74.1, 73.9, 73.2, 72.6, 72.5, 71.4, 71.3, 70.8, 63.9, 62.3, 34.8, 30.2, 30.1, 30.0, 29.9, 29.6, 27.7, 25.7. HR ESI MS positive mode: m/z calcd for $C_{43}H_{53}N_2O_{17}S$ $[M + H]^+$, 901.3065; found, 901.3084.

FRET-TDM General Storage and Use. Synthetic FRET-TDM and FITC-TMM were typically stored as a 1 mM stock solution in DMSO at −20 °C. Enzymatic and cellular assays utilized FRET-TDM at final concentrations of 1−10 μM, with the final concentration of DMSO being 1% in all samples and controls.

Commercial and Recombinant Proteins. *Msmeg* Tdmh and its catalytic mutant $Tdmh_{S124A}$ carrying His_6 tags were expressed and purified from *E. coli* as previously reported by Ojha.[21,22] *Mtb* Ag85C and its catalytic mutant $Ag85C_{S124A}$ carrying His_6 tags were expressed and purified from *E. coli* as previously reported by Ronning.[43] Purity of recombinant proteins was assessed by SDS-PAGE. Commercially available hydrolases from yeast, *P. cepacia*, *B. subtilis* esterase, and *C. rugosa* were obtained from Sigma. Porcine pancreas lipase was obtained from MP Biomedicals. Enzymatic activation of FRET-TDM was typically performed using 10 μg/mL of enzyme in HEPES buffer (50 mM HEPES, 300 mM NaCl, pH 7) or Tris buffer (50 mM Tris, 300 mM NaCl, 0.5% glycerol, pH 7.4).

In Vitro Evaluation of FRET-TDM with Tdmh, Ag85C, and Commercial Hydrolases. FRET-TDM quenching efficiency, activation by purified enzymes, and Tdmh/Ag85C kinetics were evaluated by fluorescence assays using a Tecan F200 or M200 multimodal plate reader. Excitation and emission wavelengths of 488 and 525 or 535 nm were used, respectively. Fluorescence measurements were performed in black 96-well plates. The gain setting was optimized to wells containing the fluorescent standard FITC-TMM. Fluorescence was monitored continuously and mean fluorescence intensities are reported in arbitrary units (a.u.).

For the quenching efficiency experiments, varying concentrations of FRET-TDM (0.1−10 μM) and the fluorescent standard FITC-TMM were prepared in Tris buffer with a final DMSO concentration of 1% in a black 96-well plate. Fluorescence measurements were taken as described above and fluorescence versus probe concentration plots were used to calculate quenching efficiency as described previously.[44]

For evaluation of FRET-TDM activation by commercial and recombinant enzymes (acquired as described above), 10 μg/mL of enzyme was incubated in the presence of FRET-TDM (10 μM) in Tris buffer at 37 °C in black 96-well plates. The final concentration of DMSO was 1%. Reactions were initiated by addition of the enzyme to a mixture of buffer and FRET-TDM. After thorough mixing, fluorescence was monitored continuously as described above, typically over 12−16 h.

For determination of kinetic parameters, recombinant *Msmeg* Tdmh or *Mtb* Ag85C (each used at 500 nM) was incubated in the presence of varying concentrations of FRET-TDM (0.01−50 μM) in HEPES buffer at 37 °C in black 96-well plates. The final concentration of DMSO was 1%. Reactions were initiated by addition of the enzyme to a mixture of buffer and FRET-TDM. After thorough mixing, fluorescence was monitored continuously as described above over 5 min, during which the fluorescence signal increase was linear. Relative fluorescence units were converted to FITC-TMM concentration values using a standard curve constructed from a dilution series of the fluorescent standard FITC-TMM measured in the same microplate. Product concentration versus time plots were constructed and initial velocities at each tested probe concentration were determined. From these data, GraphPad Prism v. 6.02 was used to obtain Michaelis−Menten plots and kinetic parameters.

For MS analysis of FRET-TDM hydrolysis by Tdmh, FRET-TDM (670 μM) was incubated in the presence or absence of Tdmh (10 μg/mL) in Tris buffer at 37 °C for 24 h. The sample and control were treated with an equal volume of cold acetone and then centrifuged at 3000 rpm for 5 min. The supernatants were diluted 10-fold with CH_3CN/H_2O 1:1 (v/v) containing 0.1% formic acid and analyzed by ESI-MS in positive mode using a Waters LCT Premier XE mass spectrometer.

Bacterial Strains, Growth Conditions, and FRET-TDM Cellular Assays. See Table S1 for mycobacterial strains used in this study. *Msmeg* mc^2155 strains were cultured in M63 medium (0.5% casamino acids, 2% glucose, 1 mM $MgSO_4$, 0.7 mM $CaCl_2$) with 0.05% Tween-80 or Middlebrook 7H9 liquid medium supplemented with albumin-dextrose-catalase (ADC), 0.5% glycerol, and 0.05% Tween-80. For attenuated *Mtb* mc^27000 strains, ADC was replaced with OADC (contains oleic acid), and 100 μg/mL pantothenic acid was added in 7H9 broth or plate cultures. When necessary, hygromycin and kanamycin were added at 50−150 or 20 μg/mL to culture mutants and the complemented strains, respectively. Other bacterial strains used included *C. glutamicum* 534, *E. coli* K12 MG1655, and *B. subtilis* 168. *Msmeg* wild type stocks were from the Swarts lab. *C. glutamicum*, *E. coli*, and *B. subtilis* stocks were from the Siegrist lab (University of Massachusetts, Amherst). *C. glutamicum*, *E. coli*, and *B. subtilis* were cultured in LB liquid medium.

For FRET-TDM experiments in *Msmeg* mc^2155, Δ*MSMEG_1529*, and its complementary strain Δ*MSMEG_1529comp*, bacteria from a freshly streaked plate were inoculated in 7H9 with ADC or M63 medium, with 0.05% (v/v) Tween-80 present in both conditions. After reaching exponential phase, cultures were harvested and washed with PBS 1× containing 0.5% bovine serum albumin (PBSB). Cells were resuspended in fresh medium (7H9 with ADC or M63) and normalized to OD_{600} = 1.0. 198 μL of cultures were mixed with 2 μL probe (giving a final probe concentration of 10 μM and a final DMSO concentration of 1%) in black 96-well plates and fluorescence was continuously monitored at 37 °C (excitation 488/emission 535) using a Tecan F200 or M200 multimodal plate reader. For assays with starved cultures, exponential phase cultures grown in M63 with 0.05% (v/v) Tween-80 were harvested and washed once with PBS and then starved in PBS for the desired time before the assay process was initiated.

For FRET-TDM experiments in *Mtb* mc^27000 (a severely attenuated derivative of H37Rv lacking *panCD* and *RD1* loci) and its associated strains, bacteria were inoculated in Sauton's

DOI: 10.1021/acsomega.9b00130
ACS Omega 2019, 4, 4348−4359

medium with 0.05% (v/v) Tween-80 and 100 μg/mL pantothenic acid. Exponential phase cultures were harvested and washed once with PBS 1× containing 0.05% Tween-80 (PBST). Cells were resuspended in fresh Sauton's medium with 0.05% (v/v) Tween-80 and 100 μg/mL pantothenic acid and normalized to OD_{600} = 1.0. 198 μL of cultures were mixed with 2 μL probe (giving a final probe concentration of 10 μM and a final DMSO concentration of 1%) in black 96-well tissue culture-treated plates (Falcon #353219) and fluorescence reads were collected using a BioTek Ultra microplate reader FLx800 with excitation 485 nm and emission 540 nm. For assays involving induction of $Tdmh_{Msmeg}$ in mc^27000:$\Delta tdmh_{Mtb}$, 0.2% succinate and 0.2% acetamide were added to exponential phase cultures of mc^27000:$\Delta tdmh_{Mtb}$:*pAO10* or its corresponding empty vector control strain mc^27000:$\Delta tdmh_{Mtb}$:*pLAM12* to induce $Tdmh_{Msmeg}$ expression for 4 days before the assay process was initiated. For assays with starved cultures, exponential phase cultures grown in 7H9 with OADC were harvested and washed once with PBST, then starved in PBST for the desired time before the assay process was initiated.

FRET-TDM Native PAGE Assays. *Msmeg* strains were cultured in M63 medium until exponential phase and then pelleted by centrifugation (cells pellets were stored at −80 °C if needed). Cell pellets were resuspended in 1 mL of lysis buffer (50 mM Tris, 300 mM NaCl, 0.5 mM $CaCl_2$, 0.5 mM $MgCl_2$, 0.2% (v/v) Triton X-100). The resuspended cells were then transferred to screw-top microcentrifuge tubes containing ∼0.25 mL of 0.1 mm silica beads. The cells were mechanically lysed with an MP Biomedicals FastPrep-24 bead beater, three times at 5.0 m/s for 20 s. Between each cycle, the cells were cooled on ice for 5 min. The lysates were transferred into 15 mL centrifuge tubes and centrifuged at 3000 rpm for 5 min. The supernatants were collected and transferred to new tubes, and the protein concentration was determined by Bradford assay using BSA as a standard to facilitate equal protein loading onto native gels.

For gel electrophoresis, 5−10 μg proteins were resolved on a 7.6% Tris-native gel containing 25% glycerol with no SDS. Protein samples were mixed with 3 μL of 6× sample loading buffer without SDS (250 mM Tris-HCl, pH 6.8, 60% glycerol, 0.02% w/v bromophenol blue). The sample volumes were adjusted to 25 μL with Milli-Q water and loaded onto the gels. The proteins were resolved by electrophoresis using 1× Tris-glycine running buffer without SDS at constant voltage of 100 V for 4 h in a cold room (4 °C). The running buffer was kept cold by using an ice pack. After electrophoresis, the gels were rinsed with prechilled Milli-Q water and then treated for less than 30 s with 500 μL of 10 μM FRET-TDM in 1× PBS (prepared from 1 mM DMSO stock). In-gel fluorescence was detected with a Typhoon FLA 7000 (GE Healthcare Life Science) using the fluorescein excitation/emission filter. Identical gels run in parallel, but not treated with FRET-TDM, were fixed for 15 min (40% ethanol, 10% acetic acid in water), washed three times, 5 min each with Milli-Q water, and then stained overnight at room temperature with gentle agitation in QC Colloidal Coomassie stain (Bio-Rad). The gels were destained in water for 3 h, changing the water each hour. The Coomassie-stained gel was imaged using a ChemiDoc Touch Imaging System (Bio-Rad) and processed by Image Lab software version 6.0 (Bio-Rad).

■ ASSOCIATED CONTENT

Supporting Information

The Supporting Information is available free of charge on the ACS Publications website at DOI: 10.1021/acsomega.9b00130.

Synthesis of FITC-TMM; background fluorescence of FRET-TDM in various buffers and media; optimization of FRET-TDM and Tdmh concentrations; list of mycobacterial strains used in this study; FRET-TDM activation analysis; and NMR spectra (PDF)

■ AUTHOR INFORMATION

Corresponding Author

*E-mail: ben.swarts@cmich.edu.

ORCID

Donald R. Ronning: 0000-0003-2583-8849

Benjamin M. Swarts: 0000-0001-8402-359X

Author Contributions

⊥N.J.H. and H.W.K. contributed equally to this work.

Notes

The authors declare no competing financial interest.

■ ACKNOWLEDGMENTS

B.M.S. was supported by a National Science Foundation CAREER Award (1654408) and a Henry Dreyfus Teacher-Scholar Award from The Camille & Henry Dreyfus Foundation (TH-17-034). A.K.O. was supported by the National Institutes of Health (R01AI132422) and the Wadsworth Center. D.R.R. was supported by the National Institutes of Health (R01AI105084) and the University of Toledo. Dr. Wenyan Xu is thanked for assistance with kinetic analyses and Dr. Robin J. Hood is thanked for assistance with NMR and MS instrumentation.

■ REFERENCES

(1) Hoffmann, C.; Leis, A.; Niederweis, M.; Plitzko, J. M.; Engelhardt, H. Disclosure of the Mycobacterial Outer Membrane: Cryo-Electron Tomography and Vitreous Sections Reveal the Lipid Bilayer Structure. *Proc. Natl. Acad. Sci. U.S.A.* **2008**, *105*, 3963−3967.

(2) Zuber, B.; Chami, M.; Houssin, C.; Dubochet, J.; Griffiths, G.; Daffe, M. Direct Visualization of the Outer Membrane of Mycobacteria and Corynebacteria in Their Native State. *J. Bacteriol.* **2008**, *190*, 5672−5680.

(3) World Health Organization. *Global Tuberculosis Report*, 2018.

(4) Mailaender, C.; Reiling, N.; Engelhardt, H.; Bossmann, S.; Ehlers, S.; Niederweis, M. The MspA Porin Promotes Growth and Increases Antibiotic Susceptibility of Both Mycobacterium Bovis BCG and Mycobacterium Tuberculosis. *Microbiology* **2004**, *150*, 853−864.

(5) Stephan, J.; Bender, J.; Wolschendorf, F.; Hoffmann, C.; Roth, E.; Mailänder, C.; Engelhardt, H.; Niederweis, M. The Growth Rate of Mycobacterium Smegmatis Depends on Sufficient Porin-Mediated Influx of Nutrients. *Mol. Microbiol.* **2005**, *58*, 714−730.

(6) Fabrino, D. L.; Bleck, C. K. E.; Anes, E.; Hasilik, A.; Melo, R. C. N.; Niederweis, M.; Griffiths, G.; Gutierrez, M. G. Porins Facilitate Nitric Oxide-Mediated Killing of Mycobacteria. *Microbes Infect.* **2009**, *11*, 868−875.

(7) Purdy, G. E.; Niederweis, M.; Russell, D. G. Decreased Outer Membrane Permeability Protects Mycobacteria from Killing by Ubiquitin-Derived Peptides. *Mol. Microbiol.* **2009**, *73*, 844−857.

(8) Danilchanka, O.; Pires, D.; Anes, E.; Niederweis, M. The Mycobacterium Tuberculosis Outer Membrane Channel Protein CpnT Confers Susceptibility to Toxic Molecules. *Antimicrob. Agents Chemother.* **2015**, *59*, 2328−2336.

(9) Marrakchi, H.; Lanéelle, M.-A.; Daffé, M. Mycolic Acids: Structures, Biosynthesis, and Beyond. *Chem. Biol.* **2014**, *21*, 67−85.

DOI: 10.1021/acsomega.9b00130
ACS Omega 2019, 4, 4348−4359

(10) Bansal-Mutalik, R.; Nikaido, H. Mycobacterial Outer Membrane Is a Lipid Bilayer and the Inner Membrane Is Unusually Rich in Diacyl Phosphatidylinositol Dimannosides. *Proc. Natl. Acad. Sci. U.S.A.* **2014**, *111*, 4958−4963.
(11) Indrigo, J.; Hunter, R. L.; Actor, J. K. Cord Factor Trehalose 6,6′-Dimycolate (TDM) Mediates Trafficking Events during Mycobacterial Infection of Murine Macrophages. *Microbiology* **2003**, *149*, 2049−2059.
(12) Hunter, R. L.; Venkataprasad, N.; Olsen, M. R. The Role of Trehalose Dimycolate (Cord Factor) on Morphology of Virulent M. Tuberculosis in Vitro. *Tuberculosis* **2006**, *86*, 349−356.
(13) Hunter, R. L.; Olsen, M.; Jagannath, C.; Actor, J. K. Trehalose 6,6′-Dimycolate and Lipid in the Pathogenesis of Caseating Granulomas of Tuberculosis in Mice. *Am. J. Pathol.* **2006**, *168*, 1249−1261.
(14) Rao, V.; Gao, F.; Chen, B.; Jacobs, W. R., Jr.; Glickman, M. S. Trans-Cyclopropanation of Mycolic Acids on Trehalose Dimycolate Suppresses Mycobacterium Tuberculosis -Induced Inflammation and Virulence. *J. Clin. Invest.* **2006**, *116*, 1660−1667.
(15) Ishikawa, E.; Ishikawa, T.; Morita, Y. S.; Toyonaga, K.; Yamada, H.; Takeuchi, O.; Kinoshita, T.; Akira, S.; Yoshikai, Y.; Yamasaki, S. Direct Recognition of the Mycobacterial Glycolipid, Trehalose Dimycolate, by C-Type Lectin Mincle. *J. Exp. Med.* **2009**, *206*, 2879−2888.
(16) Welsh, K. J.; Hunter, R. L.; Actor, J. K. Trehalose 6,6′-Dimycolate − A Coat to Regulate Tuberculosis Immunopathogenesis. *Tuberculosis* **2013**, *93*, S3−S9.
(17) Sathyamoorthy, N.; Takayama, K. Purification and Characterization of a Novel Mycolic Acid Exchange Enzyme from Mycobacterium Smegmatis. *J. Biol. Chem.* **1987**, *262*, 13417−13423.
(18) Belisle, J. T.; Vissa, V. D.; Sievert, T.; Takayama, K.; Brennan, P. J.; Besra, G. S. Role of the Major Antigen of Mycobacterium Tuberculosis in Cell Wall Biogenesis. *Science* **1997**, *276*, 1420−1422.
(19) Dautin, N.; de Sousa-d'Auria, C.; Constantinesco-Becker, F.; Labarre, C.; Oberto, J.; de la Sierra-Gallay, I. L.; Dietrich, C.; Issa, H.; Houssin, C.; Bayan, N. Mycoloyltransferases: A Large and Major Family of Enzymes Shaping the Cell Envelope of Corynebacteriales. *Biochim. Biophys. Acta, Gen. Subj.* **2017**, *1861*, 3581−3592.
(20) Barry, C. S.; Backus, K. M.; Barry, C. E.; Davis, B. G. ESI-MS Assay of M. Tuberculosis Cell Wall Antigen 85 Enzymes Permits Substrate Profiling and Design of a Mechanism-Based Inhibitor. *J. Am. Chem. Soc.* **2011**, *133*, 13232−13235.
(21) Ojha, A. K.; Trivelli, X.; Guerardel, Y.; Kremer, L.; Hatfull, G. F. Enzymatic Hydrolysis of Trehalose Dimycolate Releases Free Mycolic Acids during Mycobacterial Growth in Biofilms. *J. Biol. Chem.* **2010**, *285*, 17380−17389.
(22) Yang, Y.; Bhatti, A.; Ke, D.; Gonzalez-Juarrero, M.; Lenaerts, A.; Kremer, L.; Guerardel, Y.; Zhang, P.; Ojha, A. K. Exposure to a Cutinase-like Serine Esterase Triggers Rapid Lysis of Multiple Mycobacterial Species. *J. Biol. Chem.* **2012**, *288*, 382−392.
(23) Yang, Y.; Kulka, K.; Montelaro, R. C.; Reinhart, T. A.; Sissons, J.; Aderem, A.; Ojha, A. K. A Hydrolase of Trehalose Dimycolate Induces Nutrient Influx and Stress Sensitivity to Balance Intracellular Growth of Mycobacterium Tuberculosis. *Cell Host Microbe* **2014**, *15*, 153−163.
(24) Siegrist, M. S.; Swarts, B. M.; Fox, D. M.; Lim, S. A.; Bertozzi, C. R. Illumination of Growth, Division and Secretion by Metabolic Labeling of the Bacterial Cell Surface. *FEMS Microbiol. Rev.* **2015**, *39*, 184−202.
(25) O'Neill, M. K.; Piligian, B. F.; Olson, C. D.; Woodruff, P. J.; Swarts, B. M. Tailoring Trehalose for Biomedical and Biotechnological Applications. *Pure Appl. Chem.* **2017**, *89*, 1223−1249.
(26) Backus, K. M.; Boshoff, H. I.; Barry, C. S.; Boutureira, O.; Patel, M. K.; D'Hooge, F.; Lee, S. S.; Via, L. E.; Tahlan, K.; Barry, C. E., 3rd; Davis, B. G. Uptake of Unnatural Trehalose Analogs as a Reporter for Mycobacterium Tuberculosis. *Nat. Chem. Biol.* **2011**, *7*, 228−235.
(27) Swarts, B. M.; Holsclaw, C. M.; Jewett, J. C.; Alber, M.; Fox, D. M.; Siegrist, M. S.; Leary, J. A.; Kalscheuer, R.; Bertozzi, C. R. Probing the Mycobacterial Trehalome with Bioorthogonal Chemistry. *J. Am. Chem. Soc.* **2012**, *134*, 16123−16126.
(28) Rodriguez-Rivera, F. P.; Zhou, X.; Theriot, J. A.; Bertozzi, C. R. Visualization of Mycobacterial Membrane Dynamics in Live Cells. *J. Am. Chem. Soc.* **2017**, *139*, 3488−3495.
(29) Rodriguez-Rivera, F. P.; Zhou, X.; Theriot, J. A.; Bertozzi, C. R. Acute Modulation of Mycobacterial Cell Envelope Biogenesis by Front-Line Tuberculosis Drugs. *Angew. Chem., Int. Ed.* **2018**, *57*, 5267−5272.
(30) Kamariza, M.; Shieh, P.; Ealand, C. S.; Peters, J. S.; Chu, B.; Rodriguez-Rivera, F. P.; Sait, M. R. B.; Treuren, W. V.; Martinson, N.; Kalscheuer, R.; Kana, B.; Bertozzi, C. R. Rapid Detection of Mycobacterium Tuberculosis in Sputum with a Solvatochromic Trehalose Probe. *Sci. Transl. Med.* **2018**, *10*, eaam6310.
(31) Rundell, S. R.; Wagar, Z. L.; Meints, L. M.; Olson, C. D.; O'Neill, M. K.; Piligian, B. F.; Poston, A. W.; Hood, R. J.; Woodruff, P. J.; Swarts, B. M. Deoxyfluoro-D-Trehalose (FDTre) Analogues as Potential PET Probes for Imaging Mycobacterial Infection. *Org. Biomol. Chem.* **2016**, *14*, 8598−8609.
(32) Peña-Zalbidea, S.; Huang, A. Y.-T.; Kavunja, H. W.; Salinas, B.; Desco, M.; Drake, C.; Woodruff, P. J.; Vaquero, J. J.; Swarts, B. M. Chemoenzymatic Radiosynthesis of 2-Deoxy-2-[(^{18})F]Fluoro-d-Trehalose ([(^{18})F]-2-FDTre): A PET Radioprobe for in Vivo Tracing of Trehalose Metabolism. *Carbohydr. Res.* **2019**, *472*, 16−22.
(33) Foley, H. N.; Stewart, J. A.; Kavunja, H. W.; Rundell, S. R.; Swarts, B. M. Bioorthogonal Chemical Reporters for Selective in Situ Probing of Mycomembrane Components in Mycobacteria. *Angew. Chem., Int. Ed.* **2016**, *55*, 2053−2057.
(34) Kavunja, H. W.; Piligian, B. F.; Fiolek, T. J.; Foley, H. N.; Nathan, T. O.; Swarts, B. M. A Chemical Reporter Strategy for Detecting and Identifying O-Mycoloylated Proteins in Corynebacterium. *Chem. Commun.* **2016**, *52*, 13795−13798.
(35) Fiolek, T. J.; Banahene, N.; Kavunja, H. W.; Holmes, N. J.; Rylski, A. K.; Pohane, A. A.; Siegrist, M. S.; Swarts, B. M. Engineering the Mycomembrane of Live Mycobacteria with an Expanded Set of Trehalose Monomycolate Analogues. *ChemBioChem* **2018**, DOI: 10.1002/cbic.201800687.
(36) Hodges, H. L.; Brown, R. A.; Crooks, J. A.; Weibel, D. B.; Kiessling, L. L. Imaging Mycobacterial Growth and Division with a Fluorogenic Probe. *Proc. Natl. Acad. Sci. U.S.A.* **2018**, *115*, 5271−5276.
(37) Sarpe, V. A.; Kulkarni, S. S. Synthesis of Maradolipid. *J. Org. Chem.* **2011**, *76*, 6866−6870.
(38) Ojha, A. K.; Baughn, A. D.; Sambandan, D.; Hsu, T.; Trivelli, X.; Guerardel, Y.; Alahari, A.; Kremer, L.; Jacobs, W. R.; Hatfull, G. F. Growth of Mycobacterium Tuberculosis Biofilms Containing Free Mycolic Acids and Harbouring Drug-Tolerant Bacteria. *Mol. Microbiol.* **2008**, *69*, 164−174.
(39) Tallman, K. R.; Beatty, K. E. Far-Red Fluorogenic Probes for Esterase and Lipase Detection. *ChemBioChem* **2014**, *16*, 70−75.
(40) Tallman, K. R.; Levine, S. R.; Beatty, K. E. Profiling Esterases in Mycobacterium Tuberculosis Using Far-Red Fluorogenic Substrates. *ACS Chem. Biol.* **2016**, *11*, 1810−1815.
(41) Cheng, Y.; Xie, J.; Lee, K.-H.; Gaur, R. L.; Song, A.; Dai, T.; Ren, H.; Wu, J.; Sun, Z.; Banaei, N.; Akin, D.; Rao, J. Rapid and Specific Labeling of Single Live Mycobacterium Tuberculosis with a Dual-Targeting Fluorogenic Probe. *Sci. Transl. Med.* **2018**, *10*, eaar4470.
(42) Marchand, C. H.; Salmeron, C.; Raad, R. B.; Meniche, X.; Chami, M.; Masi, M.; Blanot, D.; Daffe, M.; Tropis, M.; Huc, E.; Le Maréchal, P.; Decottignies, P.; Bayan, N. Biochemical Disclosure of the Mycolate Outer Membrane of Corynebacterium Glutamicum. *J. Bacteriol.* **2011**, *194*, 587−597.
(43) Goins, C. M.; Sudasinghe, T. D.; Liu, X.; Wang, Y.; O'Doherty, G. A.; Ronning, D. R. Characterization of Tetrahydrolipstatin and Stereoderivatives on the Inhibition of Essential Mycobacterium Tuberculosis Lipid Esterases. *Biochemistry* **2018**, *57*, 2383−2393.
(44) Yadav, A. K.; Shen, D. L.; Shan, X.; He, X.; Kermode, A. R.; Vocadlo, D. J. Fluorescence-Quenched Substrates for Live Cell Imaging of Human Glucocerebrosidase Activity. *J. Am. Chem. Soc.* **2015**, *137*, 1181−1189.

DOI: 10.1021/acsomega.9b00130
ACS Omega 2019, 4, 4348−4359